Hindawi
Advances in Civil Engineering
Volume 2018, Article ID 1786392, 9 pages
https://doi.org/10.1155/2018/1786392

Research Article

Seismic Stability Analysis of Saturated and Unsaturated Soil Slopes Using Permanent Displacement

Shuai Huang and Yanju Peng

Institute of Crustal Dynamics, China Earthquake Administration, Beijing 100085, China

Correspondence should be addressed to Shuai Huang; huangshuai3395@163.com

Received 20 August 2018; Revised 2 November 2018; Accepted 28 November 2018; Published 19 December 2018

Academic Editor: Hugo Rodrigues

The permanent displacement has been widely used for slope seismic stability in practical engineering; however, the effect of the dynamic pore water pressure on the saturated and unsaturated soil slopes could not be neglected. In this paper, we propose a calculation method of dynamic pore water pressure by the hollow cylinder apparatus (GCTS) which is the most advanced and complicated device in lab testing on soil dynamics. Then, based on the proposed calculation method of dynamic pore water pressure combined with the limit equilibrium and finite element methods, we introduce a simple calculation method of permanent displacement, which avoids solving complex nonlinear equations and greatly simplifies the computational effort. Shaking table test results demonstrate the effectiveness and efficiency of the simple calculation method of permanent displacement, which could rapidly assess the soil slope seismic stability considering the effect of dynamic pore water pressure.

1. Introduction

The landslide induced by earthquake is a common geological disaster. According to preliminary statistics, more than 15,000 landslides were triggered by the Wenchuan earthquake [1]. The slopes which were designed in accordance with the seismic codes were still destroyed a lot, and a series of new features appeared in slope failure. How to prevent the failure of slope under earthquake has become one of the key techniques in slope stability analysis [2, 3]. Safety factor is often used for the slope stability evaluation at present. In fact, the slope is considered to be damaged when the safety factor is less than 1. And at this time, the slope may be in a new equilibrium, which is common in practical engineering. Thus, the safety factor will not be used for further evaluation of the slope stability when it is less than 1. Fortunately, the permanent displacement of the slope is accumulated when the safety factor is less than 1. And permanent displacement could evaluate the slope stability when the safety factor is less than 1. In addition, with the further research on slope dynamic stability, the dynamic stability evaluation method using the single seismic coefficient has been found to be insufficient. The core issue of seismic resistance of geotechnical structures has gradually transformed from the strength standard into the deformation standard. The seismic design method based on deformation is currently one of the important design theories. Thus, permanent displacement is more suitable for slope seismic stability, and how to use permanent displacement for accurate assessment of the slope stability needs further research.

Different soil slopes affected by different rainfall amounts are in different groundwater levels during the earthquake or aftershocks, and the slopes suffered from a combination of factors, including earthquake and groundwater. Seismic stability evaluation methods of slopes are the core of the slope seismic stability analysis. Therefore, it is especially important to use a reasonable safety evaluation method for slope seismic stability analysis. At present, the slope stability analysis methods mainly include the quasi-static method, Newmark sliding block method, and time-history method. The quasi-static method [4] transforms the dynamic problem into a static problem by using the dynamic coefficient, which avoids the solution

of complex nonlinear equations and greatly simplifies the computational effort. The horizontal and vertical inertial forces transformed from dynamic loads act on the center of the slope gravity, and the safety factor can be calculated fast by the quasi-static method. The quasi-static method has been widely used in engineering projects and written into the regulations in many countries. However, seismic wave characteristics, such as vibration frequency and duration of earthquake, were not considered in the quasi-static method [5]. The time-history method [6] is used to analyze the dynamic property of the slope during the seismic process considering the soil dynamic property and seismic characters. And the dynamic safety factors of the slope could be calculated under earthquake. However, the instability criterion is mostly solved by statistical methods, such as the average safety coefficient method and reliability dynamic safety factor method. How to evaluate the slope stability with dynamic safety factors at different times of earthquake action needs further research. The Newmark sliding block method [7] was first put forward by Newmark, and the soil was assumed as the ideal one which is a rigid, perfectly plastic body. The yield acceleration of the landslide mass is a constant. The landslide mass tends to start sliding when the seismic accelerations exceed the yield acceleration. Then, the permanent displacement can be obtained by a double integration of the portions of the acceleration time-history exceeding the yield acceleration [8]. Rabie [9] researched the slope stability based on the quasi-static method and time-history method and found that the quasi-static method is more conservative for slope stability analysis; Lu et al. [10] researched the seismic stability of a three-dimensional slope using the permanent displacement and found that permanent displacement was more reasonable for slope stability analysis. Therefore, in this study, the seismic stability of the soil slope is evaluated by permanent displacement. Great attention will be paid to the issue of seismic stability of the saturated and unsaturated soil slopes using permanent displacement considering the influence of the groundwater level.

In recent years, a large number of landslide disaster cases especially the slope failure phenomena in the Wenchuan earthquake show that the current evaluation method of slope stability could not meet the safety performance evaluation of the slope. The design method based on deformation is one of the most important theories of seismic design [11, 12]. The study for slope stability using permanent displacement is the hot issue in slope seismic response analysis, and the traditional method for evaluating the soil slope stability has many limits. Marzorati et al. [13] and Carro et al. [14] completed the seismic and landslide zoning maps of Umbria and Marche regions with the Newmark permanent displacement prediction model. Bray and Travasarou [15] proposed a fully coupled permanent displacement calculation method considering the dynamic effect of the slope. Shenglin et al. [16] proposed an algorithm for seismic permanent displacement of the slope considering structural surface degradation. Han et al. [17] analyzed the permanent displacement of the slope and found that the variation curve of the permanent displacement has a threshold value, and the permanent displacement increased and then became stable when the acceleration values were greater than the threshold value. Liu and Kong [18] calculated the permanent displacement of the slope using discontinuous deformation analysis; however, certain simplification has been made on the method. Although some research has been done on the slope stability using the permanent displacement, the effect of the dynamic pore water pressure under earthquake on the permanent displacement was neglected. The effect of the dynamic pore water pressure on the saturated or unsaturated soil slope stability is significant [19]. Thus, a soil slope located in Inner Mongolia Autonomous Region in China was selected to investigate the seismic stability analysis using permanent displacement.

2. Calculation Model of the Slope

2.1. Establishing the Slope Model. An actual slope which is along the Zhunshuo railway in Inner Mongolia Autonomous Region in China is selected as the research object, as shown in Figure 1. The soil types of the slope are mainly sandy. The groundwater level changes with the season, and the mean water level is above 2.0 m. The slope length is 17 m, the slope height is 12 m, and the slope angle is 35°.

The slope model in reference [20] is referred and established with the finite element software MIDAS GTS NX 2018, and the height of the finite element model is twice the slope height, as shown in Figure 2. In order to reduce the error of the calculation results, the maximum finite element mesh size is smaller than 1/10∼1/8 of the input seismic wavelength. The Mohr–Coulomb constitutive model is adopted in this study. The free field boundaries are used for the model boundaries.

The calculation parameters of the slope model are obtained by the indoor test and referenced in the *Geotechnical Engineering Handbook* [21], as shown in Table 1.

2.2. Sliding Failure Evaluation Index of the Slope. By comparison of the slope codes of the earthquake-prone countries (China, Japan, European countries, and California in the United States), evaluation methods of the slope seismic stability in different specifications were determined at home and abroad, as shown in Table 2.

By comparing slope codes in different countries, we used the safety factor and permanent displacement to evaluate the slope stability, which are closer to the actuals.

2.3. Numerical Procedure. Referring to Japanese *Specifications for Highway Bridges*, we used three real recorded seismic waves, including T1-II-1 which is a far-field seismic wave, T2-II-1 which is a near-field seismic wave, and El Centro seismic wave, to analyze the slope stability, as shown in Table 3. The peak acceleration values of the three seismic waves are scaled to 0.21 g, while the frequencies remain unchanged, as shown

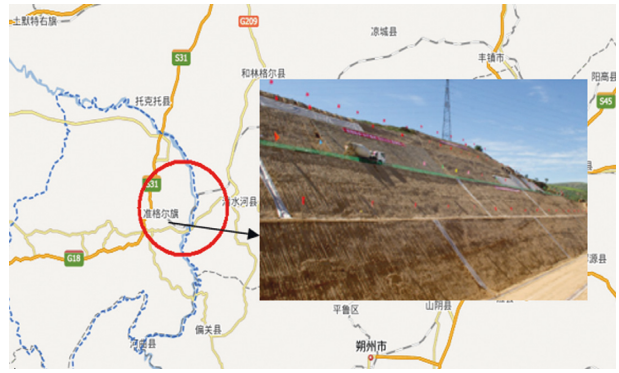

Figure 1: Engineering field figure.

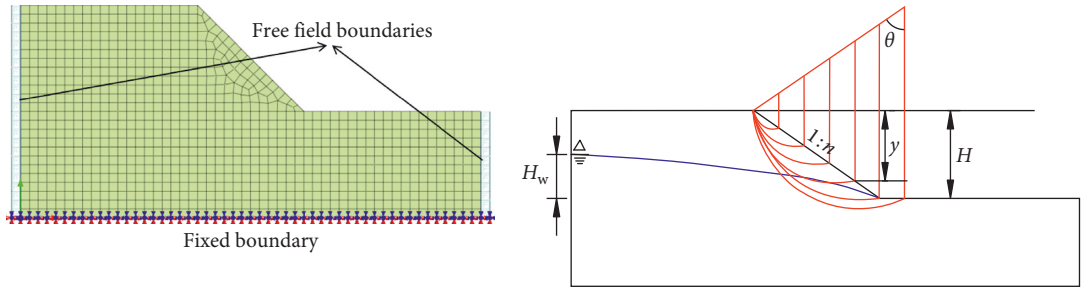

(a) (b)

Figure 2: Analysis model of the slope (reproduced from the study of Huang et al. [20], under the Creative Commons Attribution License/public domain).

Table 1: Calculation parameters of the model.

Soil type	Gravity ($kN \cdot m^{-3}$)	Poisson's ratio	Elastic modulus (MPa)	Friction angle (°)	Cohesion (kPa)	Permeability coefficient ($cm \cdot s^{-1}$)	Saturated water content (%)
Sandy	17.5	0.3	50.4	35.23	11.42	5e-5	30

Table 2: Slope codes of the earthquake-prone countries.

Nation	Codes	Evaluation methods	Evaluation indictors
China	"Technical code for building slope engineering" (GB50330-2013)	Quasi-static method [22, 23]	Safety factor
	"Design code for engineered slopes in water resources and hydropower projects" (SL386-2007)	Quasi-static method	Safety factor
	"Specifications for design of highway Subgrades" (JTG D30-2004)	Quasi-static method	Safety factor
	"Code for seismic design of railway engineering" (GB50111-2006)	Quasi-static method	Safety factor
	"Code for design on subgrade of railway" (TB10001-2005)	Quasi-static method	Safety factor
	"Code for design of high speed railway" (TB10621-2009)	Quasi-static method	Safety factor
Japan	"Design standards for railway structures"	Quasi-static method and Newmark method	Safety factor and permanent displacement
European countries	Eurocode 7: geotechnical design	Quasi-static method	Safety factor
California in the United States	California Geological Survey's guidelines (2008)	Quasi-static method	Safety factor

Table 3: Parameters of the earthquake motions.

Seismic wave	Recorded location	Earthquake name	Magnitude	Epicentral distance (km)
T1-II-1	Foundation of Itajima bridge	Hyūganada earthquake (1968)	7.5	100
El Centro	El Centro	Emperor Valley earthquake (1940)	7.7	12
T2-II-1	JR Takatori station	Kobe (1995)	7.2	16

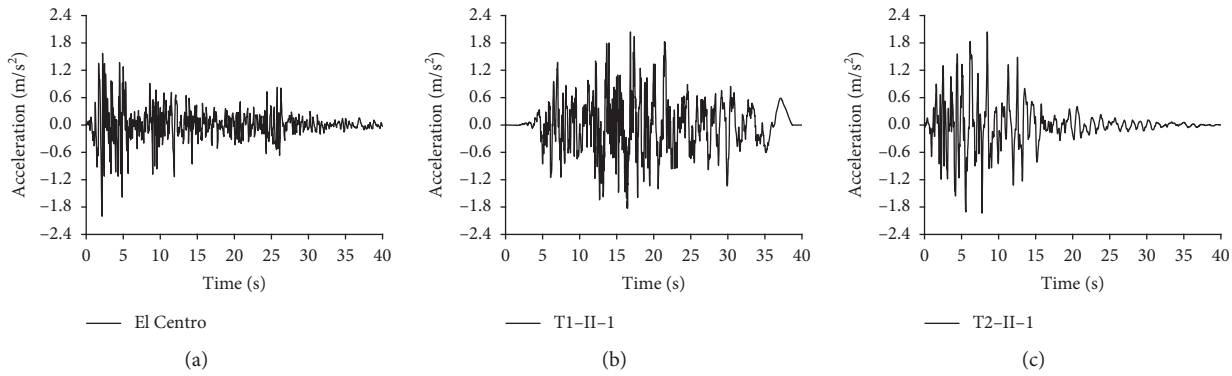

Figure 3: Time-history of earthquakes (reproduced from the study of Huang et al. [20], under the Creative Commons Attribution License/public domain).

in Figure 3. The earthquake motions are used as the horizontal excitations and input from the fixed bottom boundary.

Different factors are changed, respectively, on the basis of the original slope. Effects of various factors including slope rates, slope heights, groundwater levels, peak accelerations, and earthquake types on the safety factor and the permanent displacement of the slope are studied, as shown in Table 4.

3. Fitting Relationship of Permanent Displacement and Safety Factor

3.1. Determination of Permanent Displacement. The permanent displacement is calculated by the finite element method at a certain groundwater level considering the effect of the large deformation nonlinearity. And we calculated the permanent displacement of the slope under El Centro (2 m/s^2) at the groundwater level 5 m, as shown in Figure 4.

As shown in Figure 4, we could calculate the permanent displacement affected by different factors using the finite element method considering the effect of the large deformation nonlinearity. And the maximum permanent displacement of the slope under El Centro is 5.2 cm, when the groundwater level is 5 m.

3.2. Determination of the Safety Factor Calculation Method considering Dynamic Pore Water Pressure. Generation of the dynamic pore water pressure is mainly caused by the changes in the deviatoric stress and the average effective stress. Thus, the maximum dynamic pore water pressure could be calculated by the deviatoric stress and the average effective stress of the soil, as shown in Table 5. The dynamic hollow cylinder torsional shear test is carried out by the American dynamic hollow cylinder apparatus (GCTS), as shown in Figure 5.

Table 4: Numerical procedure.

Slope rate	Slope height (m)	Underground water level H_w (m)	Peak acceleration (m·s^{-2})	Seismic waves
1 : 1.5	12	5	2, 3, 4, 5, 6, 7, 8, 9, 10	El Centro
1 : 1.4	12	5	4, 5, 6	
1 : 1.5	12	5	4, 5, 6	El Centro
1 : 1.6	12	5	4, 5, 6	
		6	4, 5, 6	
1 : 1.5	12	7	4, 5, 6	El Centro
		8	4, 5, 6	
	12	5	4, 5, 6	El Centro
1 : 1.5	24	10	4, 5, 6	El Centro
	36	15	4, 5,6	El Centro
1 : 1.5	12	5	4, 5, 6	El Centro, T1-II-1, T2-II-1

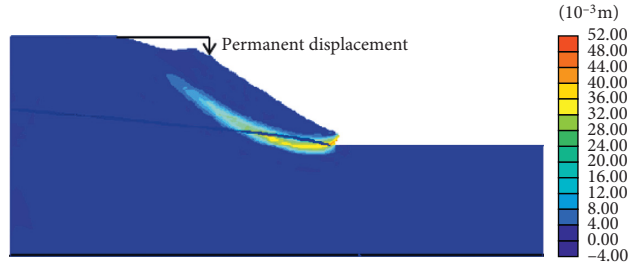

Figure 4: Permanent displacement calculated by the finite element method.

The relations of the maximum dynamic pore water pressure and the maximum deviatoric stress and the average effective stress under different earthquakes and sine waves are analyzed, as shown in Figures 5 and 6.

Table 5: Test results under earthquakes and sine waves.

Soil compaction				Working condition				
Vertical stress (kPa)	Horizontal stress (kPa)	Average effective stress (kPa)	Initial deviatoric stress (kPa)	Seismic waves	Maximum deviatoric stress (kPa)	Stress ratio	Dynamic pore water pressure (kPa)	Cycle times
300	150	200	150	T1-II-1	56.02	0.09	24	2
255	170	198	85	El Centro	51.56	0.26	25	2
300	150	200	150		62.36	0.10	29	2
255	170	198	85	T2-II-1	40.01	0.20	16	2
300	150	200	150		57.96	0.10	26	2
255	170	198	85	Sine wave 1 Hz	48.27	0.24	23	2
300	150	200	150		70.73	0.12	35	2
255	170	198	85	Sine wave 2 Hz	59.21	0.30	30	2
300	150	200	150		57.5	0.095	25	2
255	170	198	85	Sine wave 3 Hz	40.51	0.20	17	2
300	150	200	150		58.60	0.098	26	2
255	170	198	85	Sine wave 4 Hz	50.90	0.26	24	2
300	150	200	150		66.42	0.098	32	2
255	170	198	85	Sine wave 5 Hz	52.70	0.27	26	2
300	150	200	150		57.47	0.096	25	2
255	170	198	85	Sine wave 6 Hz	48.87	0.25	23	2
300	150	200	150		52.47	0.13	28	2

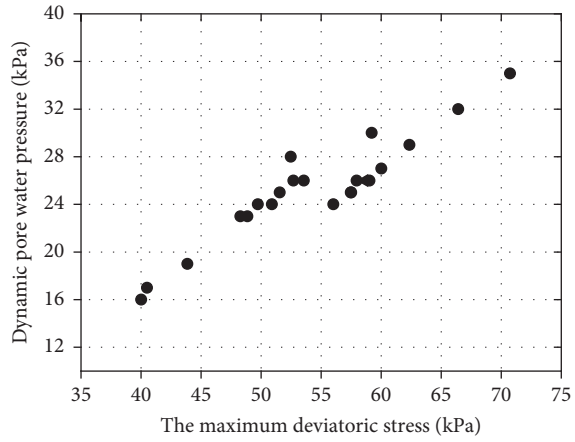

Figure 5: Relationship curve of the maximum dynamic pore water pressure and the maximum deviatoric stress.

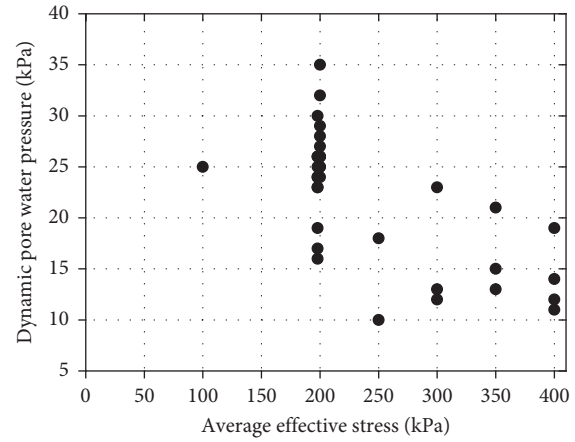

Figure 6: Relationship curve of the maximum dynamic pore water pressure and the average effective stress.

As shown in Figures 5 and 6, the maximum dynamic pore water pressure increases linearly with the increasing maximum deviatoric stress, while the maximum dynamic pore water pressure is decreasing with the increasing average effective stress.

Through the nonlinear regression analysis, the simple calculation method of the maximum dynamic pore water pressure could be obtained, as shown in the following equation:

$$\Delta u = 9 - 0.07\sigma'_{pj} + 0.7\left(\sigma'_y - \sigma'_x\right)_d, \quad (1)$$

where Δu is the maximum dynamic pore water pressure, σ'_{pj} is the average effective stress, and $(\sigma'_y - \sigma'_x)_d$ is the maximum deviatoric stress.

The simple calculation method of the maximum dynamic pore pressure is plugged into the limit equilibrium equation, and the safety factor which could consider the effect of the dynamic pore pressure is obtained, as shown in Figure 7 and equation (2).

By analyzing the stress state of the isolator in the slope, the limit equilibrium method is shown as follows:

$$F_s = \frac{\sum\{c'L(W\cos\theta - u_0 L - \Delta u L - WK_h\sin\theta)\tan\varphi\}}{\sum(W\sin\theta + WK_h\cos\theta)}, \quad (2)$$

where F_s is the safety factor; W is the weight of the free body; θ is the slope angle; φ is the internal friction angle; c' is the cohesion; L is the length of the free body parallel to the slope; u_0 is the hydrostatic pressure; Δu is the maximum dynamic pore pressure; K_h is the horizontal seismic coefficient, $K_h = a/g$; N is the normal stress of the sliding plane including the normal stress produced by $W\cos\theta$, $WK_h\sin\theta$,

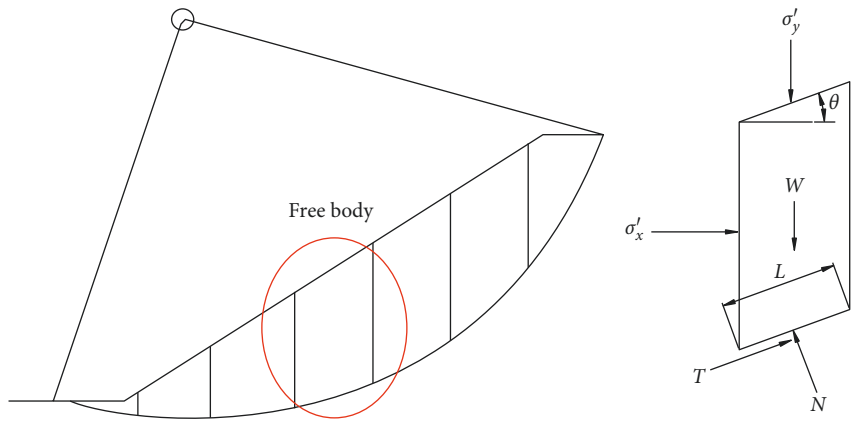

Figure 7: Stress state of a free body in the slope.

u_0, and Δu; and T is the tangential stress of the sliding plane including the tangential stress produced by $c'L$, $W \sin\theta$, and $WK_h \cos\theta$.

By using balance equation (2) of the free body, σ_y' and σ_x' could be obtained, as shown in the following equations:

$$\sigma_y' = (W\cos\theta - u_0 L) + \left(\frac{(W\sin\theta + W'\sin\theta)(1-\cos 2\theta)}{\sin 2\theta}\right), \tag{3}$$

$$\sigma_x' = (W\cos\theta - u_0 L) + \left(\frac{(W\sin\theta + W'\sin\theta)(1+\cos 2\theta)}{\sin 2\theta}\right), \tag{4}$$

where W' is the thrust of the upper soil to the lower soil.

By using equations (3) and (4), equations (5) and (6) could be obtained:

$$\sigma_{pj}' = \frac{(\sigma_y' + 2\sigma_x')}{3} = (2(W\cos\theta - u_0 L)) - \left(\frac{\{(W\sin\theta + W'\sin\theta) + 3(W\sin\theta + W'\sin\theta)\cos 2\theta\}}{\sin 2\theta}\right), \tag{5}$$

$$(\sigma_y' - \sigma_x')_d = \frac{2WK_h\cos\theta}{\sin 2\theta}. \tag{6}$$

Equations (5) and (6) are plugged into equation (1), and the maximum dynamic pore pressure Δu could be obtained. Then, Δu is plugged into equation (2), and the limit equilibrium method considering the effect of the maximum dynamic pore water pressure is obtained.

3.3. Simple Calculation Method of the Permanent Displacement. Fitting relationship of the permanent displacement and safety factor is shown in Figure 8.

As shown in Figure 8, the safety factor and the permanent displacement change exponentially with the different factors. And the permanent displacements decrease with the increasing safety factor. By fitting analysis of the permanent displacement and the safety factor, the relationship between the permanent displacement and the safety factor could be obtained.

Thus, fitting relationship of the permanent displacement and the safety factor could be obtained, as shown in the following equation:

$$\delta_{max} = 1000e^{-6.6F_s} - 2, \tag{7}$$

where δ_{max} is the permanent displacement of the slope and F_s is the safety factor of the slope.

Equation (7) considers the influence of peak acceleration, slope height, slope rate, groundwater levels, and spectrum characteristics of the seismic wave, so the permanent displacement could be calculated by this method, which could provide the reference for the seismic reinforcement of engineering designers.

4. Application Analysis of the Permanent Displacement of a Slope

In order to determine the accuracy of the proposed simple calculation method, a shaking table test of a small soil slope is carried out, as shown in Figure 9. The detailed test process can be obtained by referring to reference [20]. The groundwater levels of the slope model are 0 m, 0.6 m, 0.7 m, and 0.8 m. The length, width, and height of the model are 1.96 m, 0.96 m, and 1.4 m. The slope ratio is 1 : 1.5. We use sponge to reduce the seismic reflectance, and the sponge thickness is 20 mm.

In this study, a one-way shaking table (ES-15/KE-2000) is used for testing. There are four technical indicators in this equipment. The maximum test load and acceleration are 5000 kg and 20 m/s^2, respectively. The rated speed is 0.5 m/s. And the equipment is shown in Figure 10.

The permanent displacements are obtained from the shaking table test under T1-II-1 when the peak acceleration value is 0.4 g, as shown in Figure 11.

As shown in Figure 11, the slope starts to slide at the groundwater level 0.6 m, and the safety factor is less than 1 at this time. Permanent displacement reaches the maximum value until the groundwater level is 0.8 m. The slope

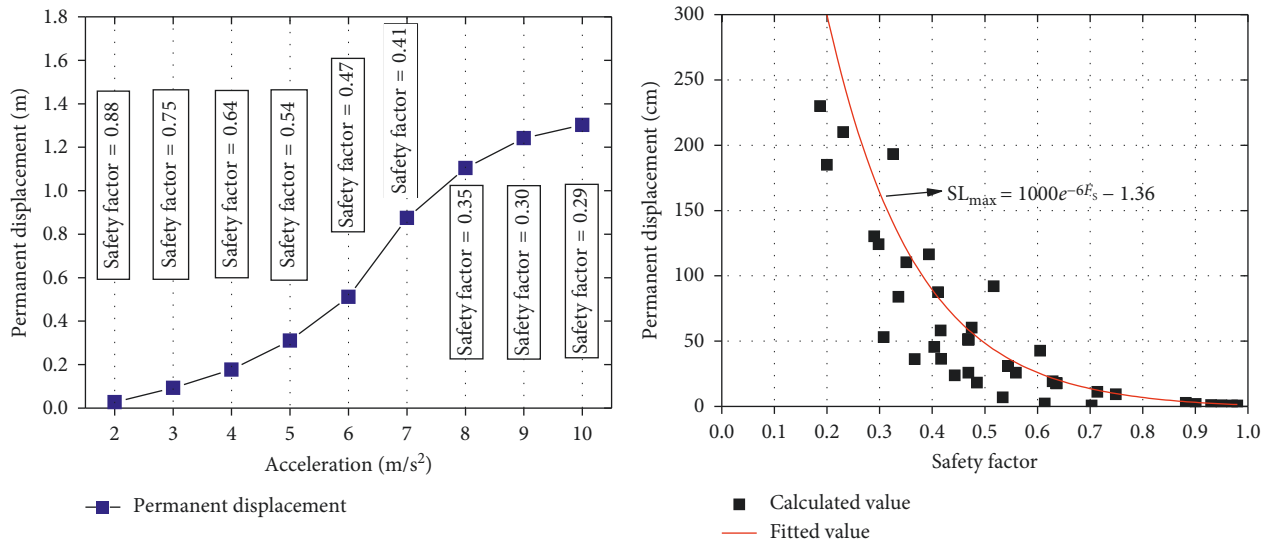

(a) (b)

Figure 8: (a) Relationship of the safety factor and the peak acceleration. (b) Fitting relationship of the permanent displacement and safety factor.

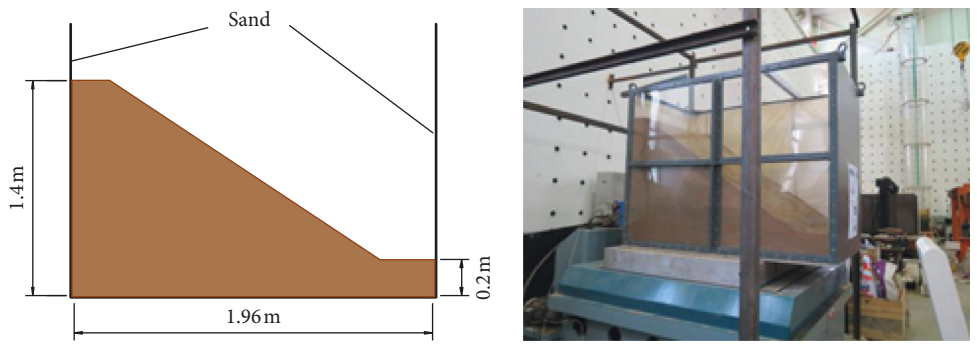

(a) (b)

Figure 9: The small slope model (reproduced from the study of Huang et al. [20], under the Creative Commons Attribution License/public domain).

(a) (b)

Figure 10: Vibration equipment (reproduced from the study of Huang et al. [20], under the Creative Commons Attribution License/public domain).

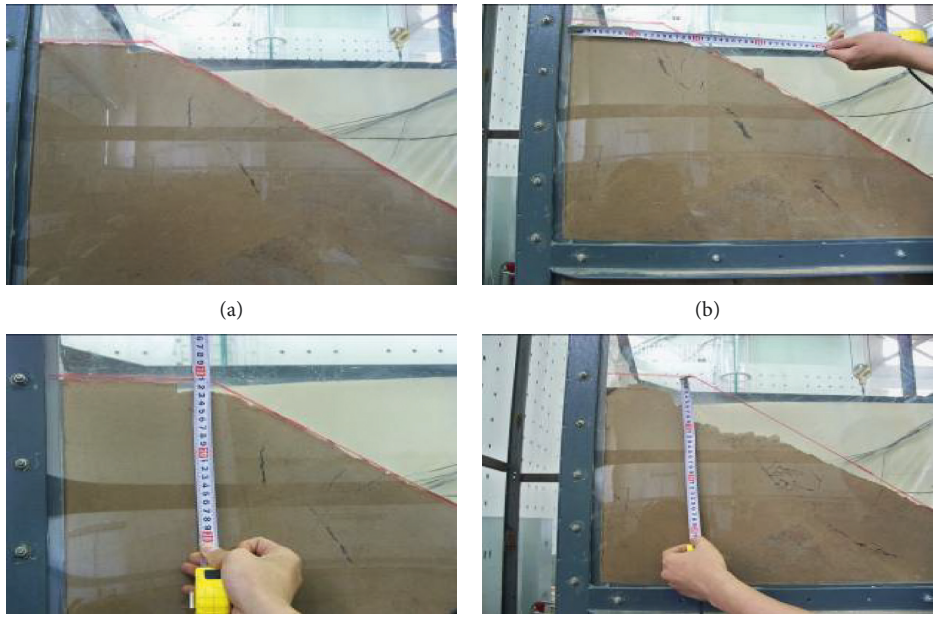

Figure 11: Permanent displacements during the test. (a) $H_w = 0$ m. (b) $H_w = 0.6$ m. (c) $H_w = 0.7$ m. (d) $H_w = 0.8$ m.

just slides but it does not collapse, and the slope is in a new equilibrium, which is usual in practical engineering. The safety factor will not be used for further evaluation of the slope stability when it is less than 1; however, the permanent displacement of the slope is accumulated. Therefore, the permanent displacement could be used for further evaluation of the slope stability. It is found that, with the increasing groundwater levels, the permanent displacement increases. The permanent displacement values will be 3.8 cm, 5.2 cm, and 8.3 cm, respectively, when the groundwater levels are 0.6 m, 0.7 m, and 0.8 m. It shows that the effect of the groundwater level on the permanent displacement should be paid more attention, and certain definitive steps should be taken to maintain the stability of the slope.

The permanent displacement obtained from the shaking table test is compared with that calculated by the simple calculation method, as shown in Figure 12.

As shown in Figure 12, the permanent displacements increase with the increasing groundwater levels. The permanent displacement obtained from the shaking table test at the groundwater level 0.8 m is about 4.0 times the permanent displacement at the groundwater level 0 m, which shows that the increase of the groundwater level has a significant effect on the permanent displacement of the slope. Also, we found that the permanent displacements obtained by the simple calculation method are greater than the permanent displacements obtained from the shaking table test. The maximum deviation value obtained from the two methods, respectively, is within 18% when the ground water level is 0.8 m. Therefore, the simple calculation method is feasible, and it could be used to calculate the permanent displacement of the soil slope in different groundwater levels.

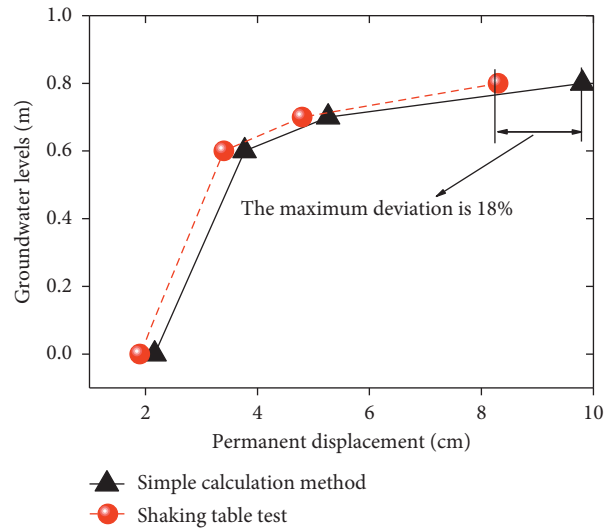

Figure 12: Permanent displacements of different methods.

5. Conclusion

The aim of this research is to lay a foundation for the stability evaluation of the saturated and unsaturated soil slopes using permanent displacement. A series of dynamic hollow cylinder torsional shear tests were conducted under different confining and deviatoric stresses, and a calculation method of dynamic pore water pressure associated with deviatoric and average effective stresses is proposed. The calculation method avoids the solution of complex nonlinear equations and greatly simplifies the computational effort.

Based on the proposed calculation method of dynamic pore water pressure combined with the limit equilibrium and finite element methods, we introduced a simple

calculation method of permanent displacement, which could provide a reference to the slope seismic reinforcement for engineering designers and be used as a rapid assessment method to the slope seismic stability. Unlike traditional calculation methods of permanent displacement, the proposed calculation method considered the effect of the dynamic pore water pressure.

The superior performance of the simple calculation method of the permanent displacement was demonstrated based on the shaking table test. The shaking table test results indicated that the calculation method could rapidly assess the seismic stability of the soil slope considering the effect of dynamic pore water pressure. The permanent displacement values obtained from the simple calculation method were greater than the permanent displacement values obtained from the shaking table test; however, the maximum deviation was within 18%, which verified the simple calculation method is feasible.

Data Availability

The data used to support the findings of this study are included within the article.

Conflicts of Interest

There are no conflicts of interest regarding the publication of this paper.

Acknowledgments

This work was financially supported by the Beijing Natural Science Foundation (Grant No. 8174078), National Natural Science Foundation of China (Grant No. 51708516), and National Key R&D Program of China (2017YFC1500404) and the research grant from Institute of Crustal Dynamics, China Earthquake Administration (No. ZDJ2016-12).

References

[1] Y. Yin, "Features of landslide striggered by the Wenchuan earthquake," *Journal of Engineering Geology*, vol. 17, no. 1, pp. 30–38, 2009.

[2] S. A. Sepúlveda, W. Murphy, R. W. Jibson, and D. N. Petley, "Seismically induced rock slope failures resulting from topographic amplification of strong ground motions: the case of pacoima canyon, California," *Engineering Geology*, vol. 80, no. 3/4, pp. 336–348, 2005.

[3] E. Eberhardt, K. Thuro, and M. Luginbuehl, "Slope instability mechanisms in dipping interbedded conglomerates and weathered marls-the 1999 Rufi landslide, Switzerland," *Engineering Geology*, vol. 77, no. 1/2, pp. 35–56, 2005.

[4] L. Liu, Z. Lei, and F. Zhou, "The evaluation of seismic slope stability analysis methods," *Journal of Chongqing Jiaotong University*, vol. 20, no. 3, pp. 83–88, 2001.

[5] Z. ping Fan and Li hua Zhang, "Analysis on slope stability during earthquake," *Northwestern Seismological Journal*, vol. 32, no. 4, pp. 339–343, 2010.

[6] H. Liu, F. Kang, and Y. Gao, "Time history analysis method of slope seismic stability," *Rock and Soil Mechanics*, vol. 24, no. 4, pp. 553–560, 2003.

[7] N. M. Newmark, "Effects of earthquakes on dams and embankments," *Géotechnique*, vol. 15, no. 2, pp. 139–160, 1965.

[8] A. Liu, Z. Lu, T. X. Liu, and L. Yang, "Study seismic slope permanent displacements with dynamic critical acceleration," *China Earthquake Engineering Journal*, vol. 39, no. 5, pp. 876–882, 2017.

[9] M. Rabie, "Comparison study between traditional and finite element methods for slopes under heavy rainfall," *HBRC Journal*, 2014, In press.

[10] K. Lu, D. Zhu, Y. Zhu et al., "Preliminary study of seismic permanent displacement of 3D slope," *Rock and Soil Mechanics*, vol. 32, no. 5, pp. 1425–1429, 2011.

[11] W. Randall, "Jibson. Methods for assessing the stability of slopes during earthquakes-A retrospective," *Engineering Geology*, vol. 122, pp. 43–50, 2011.

[12] E. M. Rathje and G. Antonakos, "A unified model for predicting earthquake-induced sliding displacements of rigid and flexible slopes," *Engineering Geology*, vol. 122, no. 1-2, pp. 51–60, 2011.

[13] S. Marzorati, L. Luzi, and M. De Amicis, "Rock falls induced by earthquakes: a statistical approach," *Soil Dynamics and Earthquake Engineering*, vol. 22, no. 7, pp. 565–577, 2002.

[14] M. Carro, M. De Amicis, L. Luzi, and S. Marzorati, "The application of predictive modeling techniques to landslides induced by earthquakes: the case study of the 26 September 1997 Umbria-Marche earthquake (Italy)," *Engineering Geology*, vol. 69, no. 1-2, pp. 139–159, 2003.

[15] J. D. Bray and T. Travasarou, "Simplified procedure for estimating earthquake-induced deviatoric slope displacements," *Journal of Geotechnical and Geoenvironmental Engineering*, vol. 133, no. 4, pp. 381–392, 2007.

[16] Q. Shenglin, Q. Shengwen, W. Faquan et al., "On permanent displacement of earthquake induced slide based on residual pushing force method," *Journal of Engineering Geology*, vol. 12, no. 1, pp. 63–68, 2004.

[17] J. Han, W. Lv, and Y. Ou, "Study on analysis method for permanent displacement of slope under seismic action," *Subgrade Engineering*, vol. 4, pp. 37–41, 2016.

[18] J. Liu and X. Kong, "Seismic stability and permanent displacement analysis of a solid waste landfill slope containing geomembrane," *Rock and Soil Mechanics*, vol. 25, no. 5, pp. 778–782, 2004.

[19] S. Malla, "Consistent application of horizontal and vertical earthquake components in analysis of a block sliding down an inclined plane," *Soil Dynamics and Earthquake Engineering*, vol. 101, pp. 176–181, 2017.

[20] S. Huang, Y. Lv, Y. Peng et al., "Permanent displacement analysis of soil slope considering dynamic pore water pressure under severe earthquakes," *Electronic Journal of Geotechnical Engineering*, vol. 20, no. 4, pp. 1529–1539, 2015s.

[21] *Geotechnical Engineering Handbook Editorial Board. Geotechnical Engineering Handbook*, China Architecture & Building Press, Beijing, China, 4th edition, 2007.

[22] S. L. Kramer, *Geotechnical Earthquake Engineering*, Prentice-Hall, Upper Saddle River, NJ, USA, 1995.

[23] H. Liu, B. Jingshan, and D. Liu, "Development on study of seismic stability evaluation methods of rock-soil slopes," *Journal of Institute of Disaster-Prevention Science and Technology*, vol. 9, no. 3, pp. 20–27, 2007.